Supporting Information (SI)

Hydrophilic mechano-bactericidal nanopillars require external forces to rapidly kill bacteria

Amin Valiei[1#], Nicholas Lin[1#], Jean-Francois Bryche[2,3], Geoffrey McKay[4], Michael Canva[2,3] , Paul G. Charette[2,3], Dao Nguyen[4,5,6], Christopher Moraes[1,7,8]* and Nathalie Tufenkji[1]*

[1]Department of Chemical Engineering, McGill University, Montréal, Québec, Canada

[2]Laboratoire Nanotechnologies Nanosystèmes (LN2), CNRS UMI-3463, Université de Sherbrooke, Sherbrooke, Québec, Canada

[3]Institut Interdisciplinaire d'Innovation Technologique (3IT), Université de Sherbrooke, Sherbrooke, Québec, Canada

[4]Meakins-Christie Laboratories, Research Institute of the McGill University Health Centre, Montréal, Québec, Canada

[5]Department of Microbiology and Immunology, McGill University, Montréal, Québec, Canada

[6]Department of Medicine, McGill University, Montréal, Québec, Canada

[7]Department of Biomedical Engineering, McGill University, Montréal, Québec, Canada

[8]Rosalind and Morris Goodman Cancer Research Center, McGill University, Montréal, Québec, Canada

[#]Authors contributed equally

*Corresponding authors

E-mail: chris.moraes@mcgill.ca; Phone: 514-398-4278

E-mail: nathalie.tufenkji@mcgill.ca; Phone: 514-398-2999

Materials and Methods

Preparation of bacterial culture

The reference *P. aeruginosa* strain PAO1 was used in our studies. Prior to each experiment, bacteria from a -80 °C glycerol stock were streaked onto an Luria-Bertani (LB, Life Technologies, USA) agar plate. Fresh bacterial cultures were grown from a single colony overnight (~15 hours) at 37 °C in 5 mL of LB broth then reinoculated at 1:1000 ratio in sterile LB broth for another ~4 hours to ensure logarithmic stage of growth at time of harvest. Bacteria were centrifuged at 3000 ×*g* for 4 minutes, then resuspended in physiological phosphate-buffered saline (PBS) to an optical density (OD600nm) of ~0.3 using a UV-visible spectrophotometer (Biomate 3S, Thermo Scientific, USA).

Live/dead assay

Bacterial suspension prepared as described above were mixed with SYTO 9 and propidium iodide from the live/dead BacLight^{TM} Bacterial Viability Kit (Molecular Probes, Inc., USA) to the concentration recommended by the manufacturer. SYTO 9 is able to penetrate cells with intact membranes (referred to as live cells) giving them green fluorescent color (exitation 480 nm/emission 500 nm) while propidium iodide stains only those cells with compromised membranes causing them to fluoresce red (excitation 490/emission 635 nm), conventionally referred to as dead/dying cells. To evaluate the cell viability in fully wet conditions, the nanopillar surfaces (NanoSi or NanoZnO) or control surface (flat silicon diced from silicon wafers with no nanostructures) was placed in a microscopy dish (Matsunami, USA) and bacterial suspension was added to cover the entire substrate. To further ensure a fully wet condition, the surface was gently shaken after introduction into the liquid medium to remove any retained air pockets within nanoscale cavities. To assess the cell viability during water evaporation, a 3 µL

droplet of stained bacteria suspended in PBS was dispensed on the surface. Next, the surface was immediately mounted on the stage of a fluorescence microscope (Olympus IX71, Japan) and the viability of bacteria was monitored using a 20× objective (UCPLFLN, numerical aperture 0.7, working distance 0.8-1.8 mm, depth of field 5.8 µm, Olympus, Japan) in real-time as demonstrated in a previous report[1]. The fraction of dead bacteria was calculated by dividing the number of red cells with the total number of green and red cells at each time point. In dry conditions, the viability of bacteria was evaluated 90 s after the passage of interface. The calculation of viability was based on the average viability determined in at least three separate locations (440 µm × 330 µm image area) on each substrate and the experiments were repeated at least three times for each type of substrate.

Scanning electron microscopy (SEM)

To evaluate the morphology of attached bacteria as closely as possible to fully wet conditions, nanopillar or control surfaces were immersed in bacterial suspensions (2 mL) in 12-well microtiter plates for 30 min to allow sufficient time for bacterial attachment. Next, the substrates were rinsed with PBS to remove loosely attached cells. The PBS rinse solution was discarded and replaced with 2.5% glutaraldehyde in PBS for chemical fixation while ensuring the substrates always remained wet. To examine the bacterial morphology immediately after water evaporation, a 5 µL droplet of bacterial suspension was placed on the surfaces and left to dry. After complete liquid evaporation, a 2.5% glutaraldehyde solution was added to cover the substrates. The chemical fixation was performed at 4 °C overnight, after which glutaraldehyde was removed and immediately replaced with increasing concentrations of ethanol (30%, 50%, 70%, 80%, 90%, 100%, 100%, 100%), allowing 10-min intervals before each exchange of ethanol. Samples were then critical point dried (CPD) with CO_2 (EM CPD030, Leica

Microsystems, Germany) and sputter-coated with 5 nm of platinum (EM ACE600 High-Resolution Sputter Coater, Leica Microsystems, Germany). Bacterial cells attached to substrates were observed by SEM (FEI Inspect F50 FE-SEM, FEI Company, USA). To evaluate the fabrication of as-synthesized NanoSi and NanoZnO, the surfaces were observed with the SEM after being sputter-coated with 5 nm of platinum.

Mechanical compression test

Stamps featuring an array of small posts, each of which were 200 µm in diameter and 100 µm in height, were fabricated with a stereolithographic 3D printer (Ember, Autodesk, USA). Stamps were rinsed with 70% ethanol, then rinsed with DI water and then dried at room temperature before use. In the compression test, we immersed NanoSi, NanoZnO and flat control samples separately in a bacterial suspension which was prepared as above. The stamps were positioned such that the posts were pointed down, towards the nanopillar surfaces. We placed calibration weights on top of each stamp to deliver a known amount of external force. This system was left for 10 min, then the weight and stamp were removed. Next, samples were picked up by forceps and gently shaken to remove excess fluid. A 5 µL droplet of live/dead BacLight solution was pipetted onto each sample followed by fluorescence imaging. The experiments were repeated three times for each sample.

NanoSi fabrication

NanoSi substrates were fabricated based on methods outlined by *Peng et al.* [1]. Briefly, silicon wafers were cleaned in acetone, then isopropanol, rinsed with de-ionized water three times then soaked in Nano-strip solution (VWR, USA) at 65 ºC for 20 min. They were then rinsed thoroughly with de-ionized water before being dipped in buffered oxide etchant (Sigma–Aldrich, USA) for 1 min. Silver nanoparticles were electroplated onto the cleaned silicon wafer by

soaking the surface in a solution of $AgNO_3$/HF ($AgNO_3$: 0.01 M, HF: 4.6 M) for 1 min. After that, the substrates were soaked for etching in a solution of $FeNO_3$/HF ($FeNO_3$: 0.135 M, HF: 4.6 M) for 45 min at room temperature. The samples were rinsed with de-ionized water and silver dendrites residues on the substrate were removed by dipping the samples in HNO_3 (7 M) for 10 min. The obtained samples were rinsed again with copious amount of de-ionized water and dried at room temperature.

NanoZnO fabrication

Hydrothermal synthesis of NanoZnO is a two-step process. First, 1 mM of zinc acetate dihydrate dissolved in anhydrous ethanol was spin-coated (2000 rpm, 30 s) onto glass microscope slides which were pre-cleaned with isopropanol and acetone and dried with nitrogen flow. The glass slides were then heated on a hotplate at 300 °C for 10 min to anneal the zinc to form a seed layer. In the second step, the glass slides were immersed vertically in an aqueous growth solution containing equimolar (25 mM) zinc nitrate hexahydrate and hexamethylenetetramine and left in an oven at 70 °C. After 24 h of growth, slides were removed and rinsed three times with de-ionized water then dried at room temperature.

Ordered nanopillar array fabrication

Two highly ordered arrays of nanopillars were fabricated on a silicon wafer via e-beam lithography. In one array, the pillar-to-pillar spacing between adjacent nanopillars was 200 nm whereas the spacing in the other array was 400 nm. The height and diameter of both arrays were 300 nm and 80 nm, respectively. First, silicon wafers were cleaned as above and two resists were spin-coated on the sample, the primer hexamethyldisilazane followed by the negative e-beam resist Ma-N 2401. The average thickness was about 500 nm. Then, e-beam lithography was performed with an adaptive dose depending on diameter, density and periodicity of the final

design with a modified Zeiss microscope (Leo 1540 XB). Following the exposure, the resist was developed by immersion in a solution of Ma-D 525. Next, the silicon surfaces were etched with an inductively coupled plasma (ICP) etching system at 20 °C in a mixture of sulfur hexafluoride and octafluorocyclobutane. The etching time was adjusted as a function of the nanopillar height (~100 nm/min). Finally, samples were cleaned with a solution of remover 1165 (Dow Chemical Company, USA) to remove the resists.

Fluorescence assay using GFP-tagged bacteria

To evaluate the activity of cells during water evaporation on nanopillars and flat surfaces, GFP-labeled *P. aeruginosa* was used. It has already been demonstrated that the decay in the expression of GFP correlates well with the loss in membrane integrity and cell death[2]. A particular feature of this technique is that, contrary to live/dead assay, it does not depend on the penetration of live/dead stains to indicate the loss in viability and as such is potemtially useful in studying bacterial viability upon drying. The first step in this test is to prepare a bacterial suspension as above. A droplet of the suspension was then placed on the nanopillar-textured or control surface, and the interaction of bacteria with the surface was monitored using a fluorescence microscope (Olympus IX71, Japan). The experiments were repeated three times for each sample. For better visibility of cells, images were converted to greyscale in ImageJ (National Institute of Health, USA) and contrast and brightness were adjusted in the images all together.

Computational simulations

Numerical simulations of a bacterium deformation on a nanopillar were performed using structural mechanics module of COMSOL Multiphysics v.5.5 (Comsol Inc., USA) in 2D-axisymmetric geometry. The bacterium was modeled as a thin elastic shell representing the cell

envelope (thickness=2.5 nm^3) with a constant internal volume to account for the incompressibility of the internal fluid. A contact boundary condition between the lower surface of the shell and the nanopillar was specified and a prescribed vertical displacement towards the nanopillar was defined for the rest of the shell external surfacs. Also a constant pressure boundary condition was assigned to the internal surfaces of bacterial shell. Stress profiles and pillar reaction forces were plotted for bacterium displacement increments. In preparing the model, we assumed a Young's modulus of 30 MPa and ultimate tensile strength of 13 MPa for the cell wall, based on published estimates[4,5], and an internal hydrostatic pressure up to 0.3 atm, a typical value for bacterial turgor pressure[6].

Transmission electron microscopy (TEM)

The nanopillars of as-synthesized NanoSi and NanoZnO surfaces were individually observed by TEM (FEI Tecnai 12 BioTwin 120 kV TEM, FEI Company, USA) after scratching the nanopillar surfaces with a razor blade.

Contact angle measurements

Static contact angles of NanoSi and NanoZnO were measured on an OCA 20 contact angle analyzer (DataPhysics Instruments, Germany) equipped with automated drop delivery and digital camera. The measurements were performed in ambient temperature using the sessile drop method. A 3 μL water droplet was dispensed on the surface of each sample and the contact angle was measured after 3 s. All experiments were repeated three times and the average value of contatct angle was reported.

Supplementary Tables

Table S1. NanoSi and NanoZnO nanopillar dimesions

	Diameter (nm)	Height (nm)	Spacing (nm)
NanoSi	50±10	~900	447±395
NanoZnO	230±65	~1200	408±392

Supplementary Figures

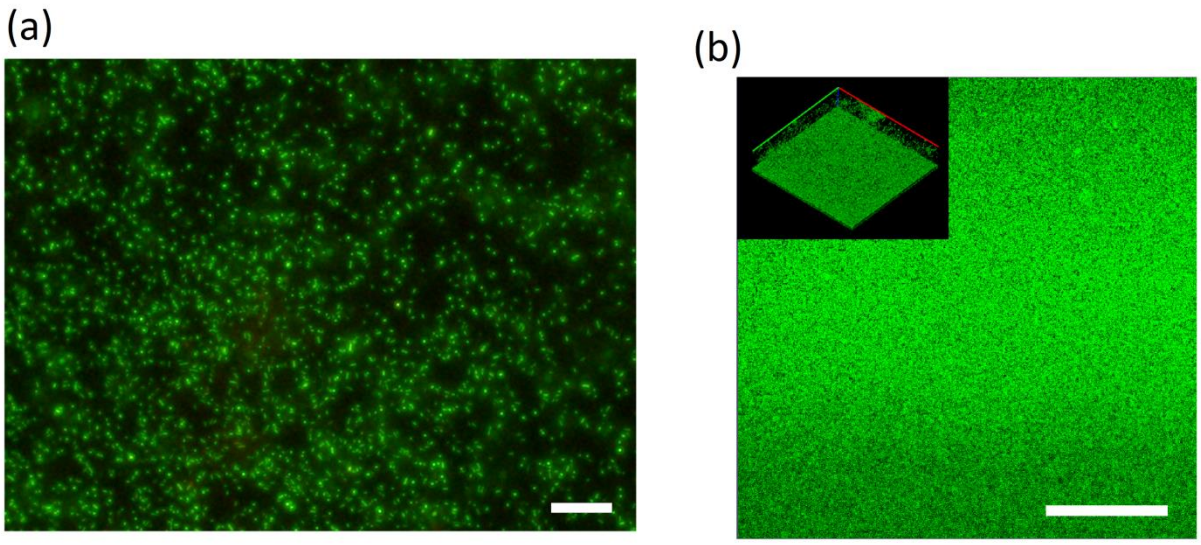

Figure S1. (a) Viability of bacteria on NanoZnO after 1 h in the fully wet condition. The majority of cells retained green fluorescence and did not uptake red fluorescence, indicating they remain viable (scale bar = 20 µm). (b) Viability of bacteria on NanoSi after 24 hour in LB broth. The bacteria form a layer of viable biofilm on the surface (scale bar = 100 µm).

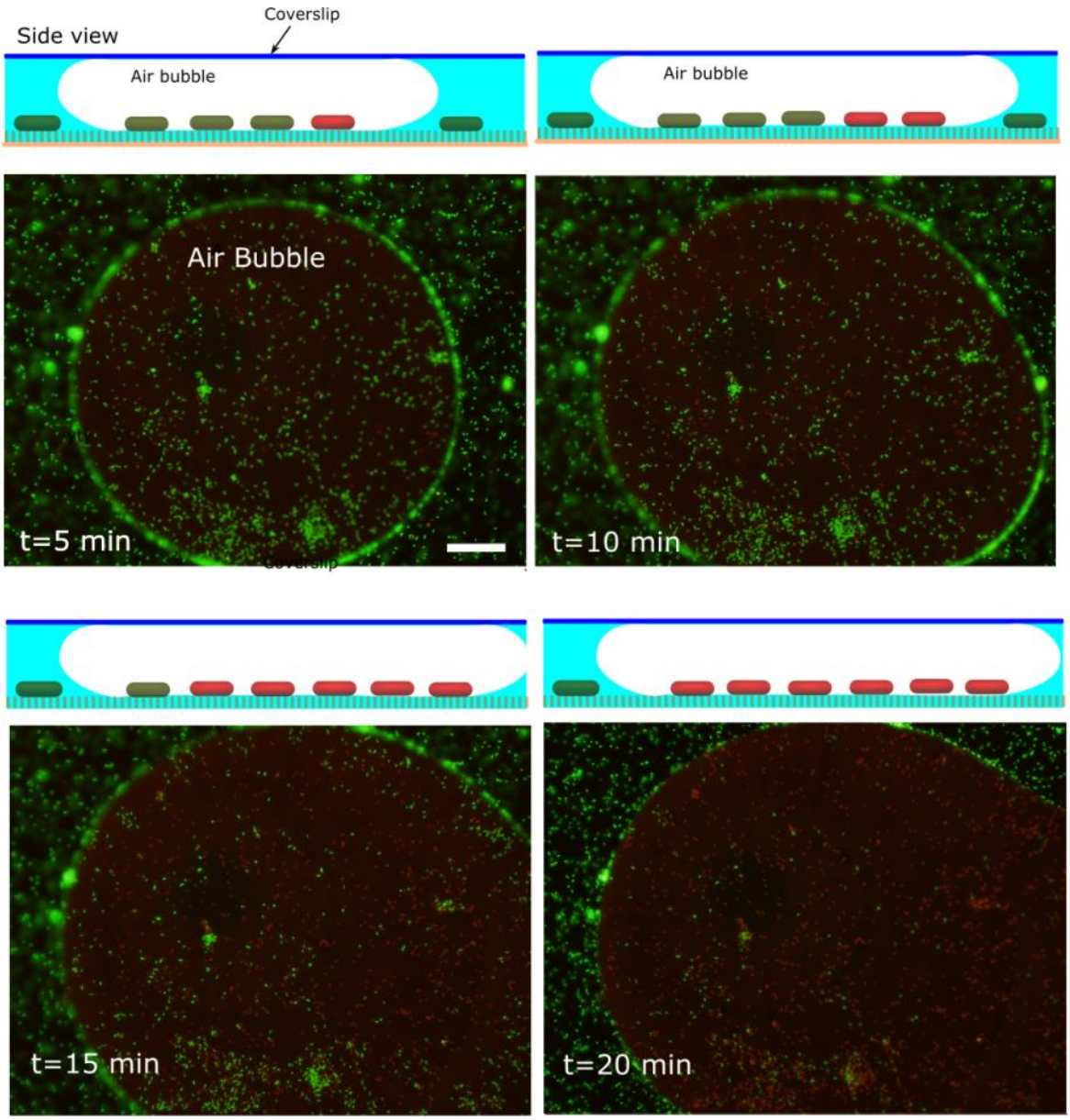

Figure S2. Viability of bacteria after the formation of an air bubble inside the confined space between NanoSi and a coverslip (scale bar = 50 µm). Top schematics above each image shows a side view of the possible bacterial killing process in a microbubble in the confined space. More than 50% of the population loses its viability in 5 min and more than 99% within 20 min of microbubble formation. The bacterial killing inside the microbubble is caused by capillary force due to the formation of air/liquid interface and subsequent liquid evaporation. It must be noted that the rate of water evaporation in this case is substantially smaller than a surface freely exposed to ambient due to the relatively small volume of air in the microbubble.

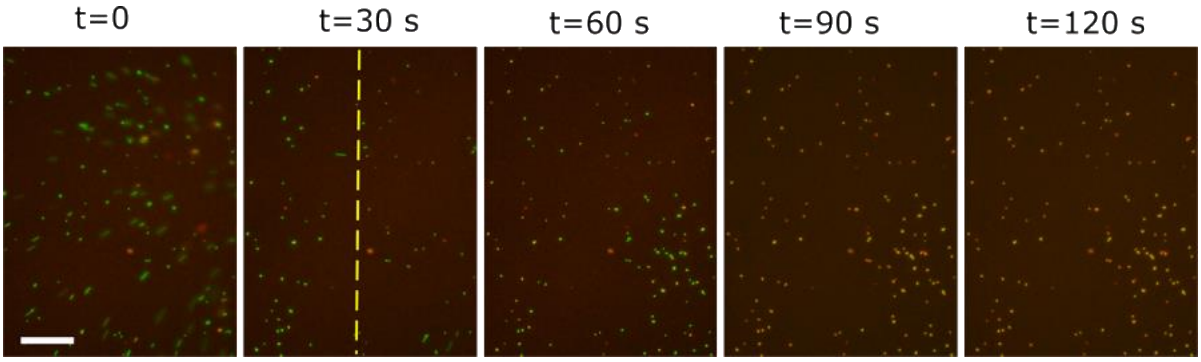

Figure S3. Viability of bacteria with time on NanoZnO upon passage of air/liquid interface (yellow line) during water evaporation (scale bar = 20 µm).

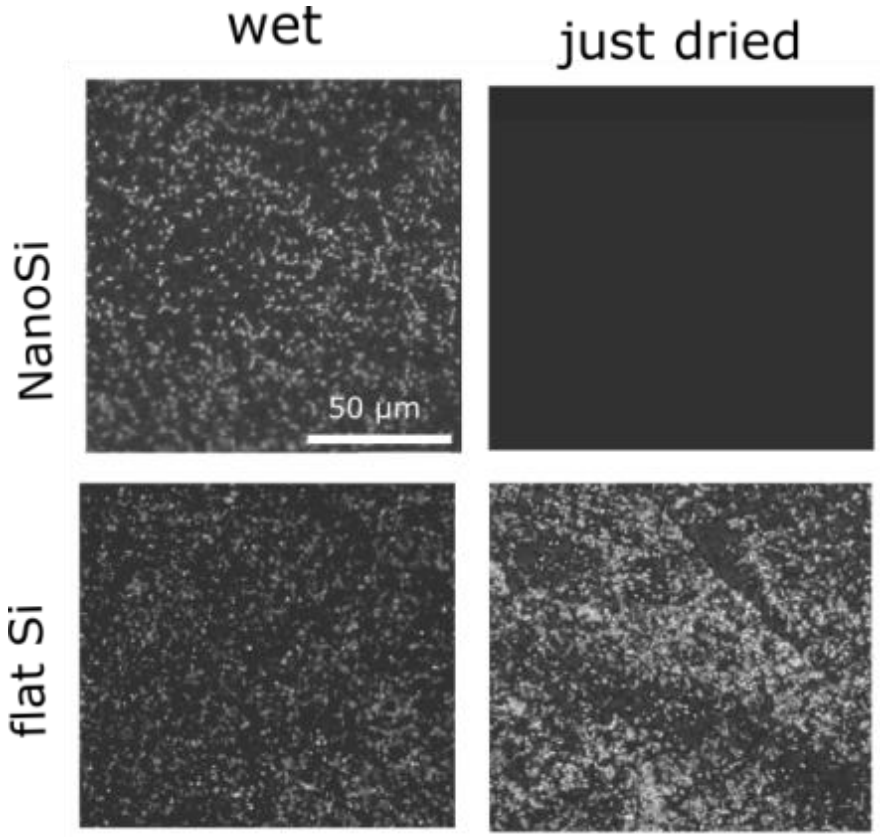

Figure S4. Fluorescent images of GFP-tagged *P. aeruginosa* on NanoSi and control (flat) Si in the wet condition and just after water evaporation. On wet NanoSi and NanoZnO surfaces, bacteria fluoresce green however, the bacterial fluorescence almost entirely vanishes after evaporation of liquid on the surface. On the control surface, attached and suspended bacteria fluoresced green in wet condition and remained fluorescent after liquid evaporation. According to Lowder *et al.*[2], the loss of bacterial GFP signal is indicative of loss in viability and could signify severe damage to cell membrane. The disappearance of GFP-signal, which is integral to cells, confirms that cell death observed in the live/dead assay is not caused by any artifacts relating to stains. In combination, both the live/dead and GFP assays demonstrate a rapid bactericidal mechanism on nanopillar surfaces upon water evaporation.

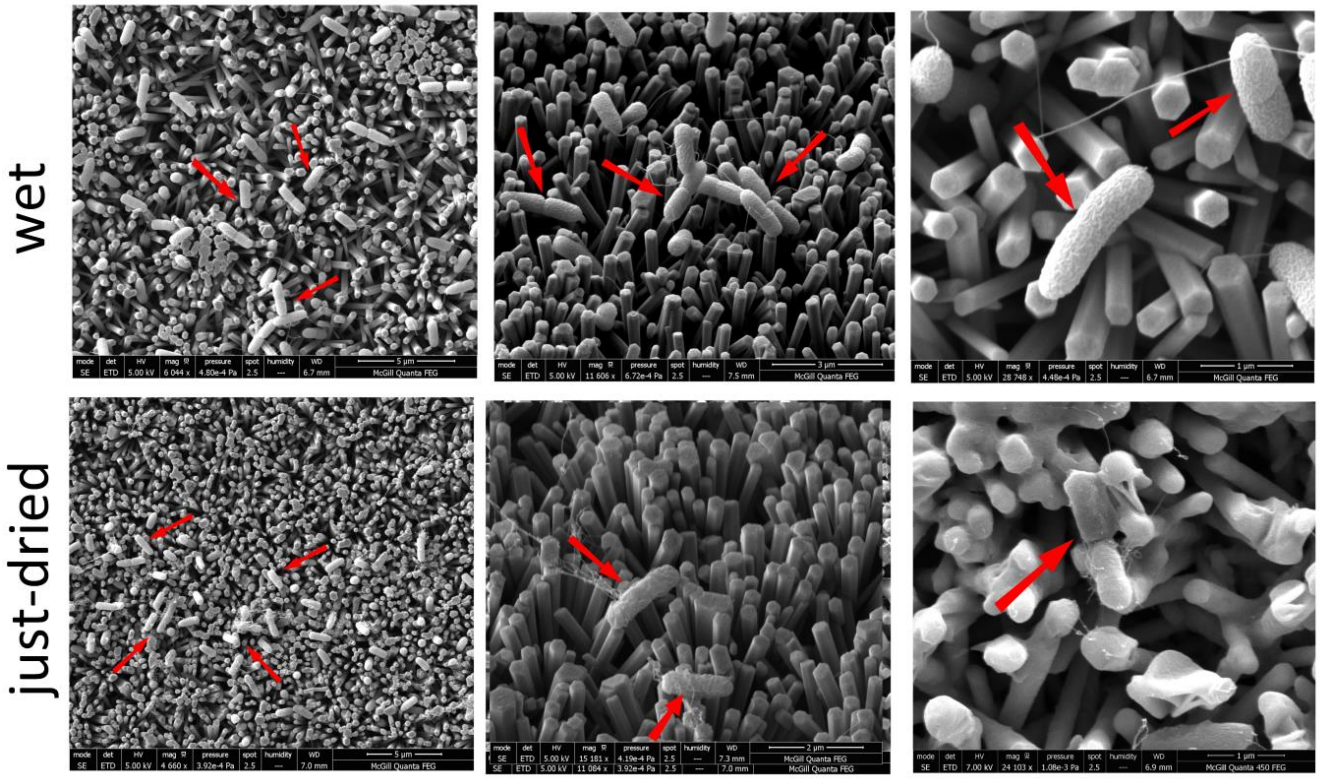

Figure S5. SEM of bacteria on NanoZnO in the wet condition and immediately after the liquid evaporation. Red arrows show the location of bacteria.

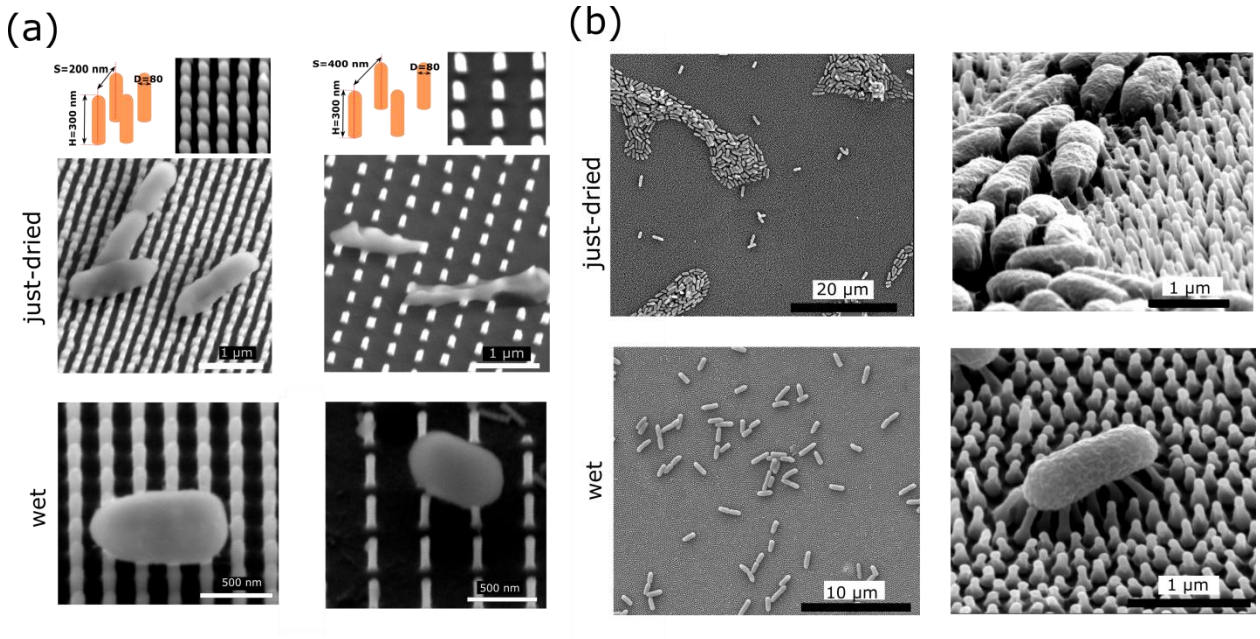

Figure S6. SEM images of bacterial morphology in the immersed wet state, where surfaces are not exposed to air during sample preparation, and the just-dried state on (a) two different ordered nanopillar arrays **(**dimension of each shown above the images). The extent of damage is greater on the pattern with larger spacing between the pillars. This is consistent with the theory of external forces. As the pillar array becomes denser the reaction to the external capillary force get smaller leading to less severe damage; (b) cicada *Salvazana mirabili*s (diameter = 90 nm, height = 300 nm, center to center spacing = 270 nm). We observe that bacterial structures are intact in the wet state for all the surfaces but damaged immediately after water evaporation. We did not pursue a comprehensive live/dead analysis for these surfaces due to limitation in sample supply for cicada wings and small pattern area (200 µm × 200 µm) for ordered nanopillar arrays.

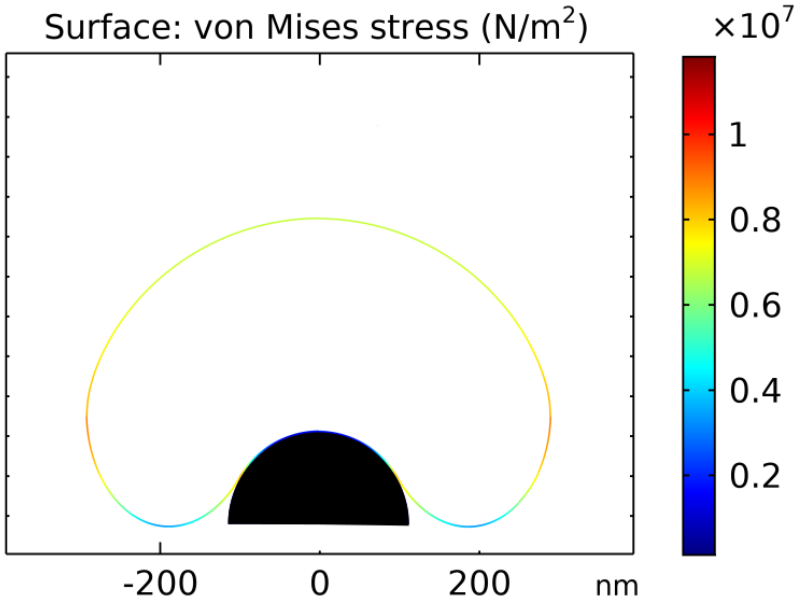

Figure S7. Stress profile of a bacterial envelope on a NanoZnO pillar. The force required to achieve the maximum von-Mises stress of 13 MPa (equal to the cell envelope ultimate tensile strength) is 6.7×10^{-9} N, higher than the calculated value for NanoSi in Fig. 4. The following parameters were used in the simulations: cell wall thickness = 2.5 nm[4], Young's modulus = 30 MPa[5,6], ultimate tensile stress 13 MPa[5], bacterial turgor pressure 0.3 atm[6] (for more information on the simulation refer to SI methods)

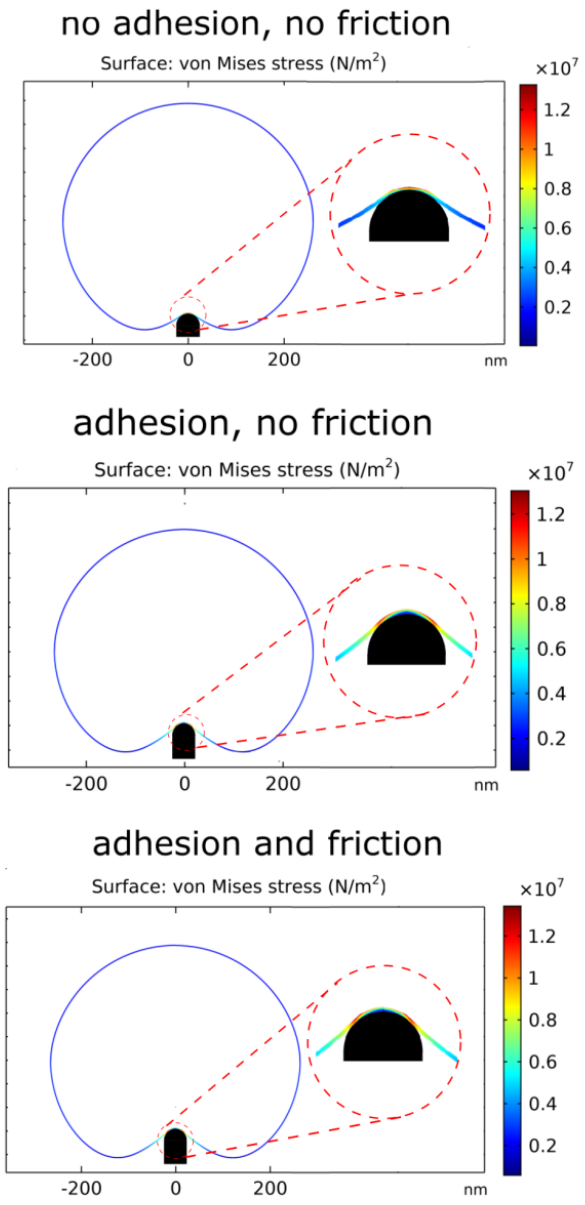

Figure S8. Stress profile of bacterial envelope obtained based on different assumptions of adhesion and friction. A friction factor of 0.1 is used for the case that involves friction[3]. The distribution of stress is different in the presence and absence of adhesion. In adhesion mode (both with and without friction), the stress is maximum at the point of detachment of the cell from nanopillar. In the no adhesion condition, the stress is maximum at the apex of the pillar (adhesion and no. friction case is the same as Figure 4).

As seen in the Table S2, the force required to deform bacteria in the adhesion (sticking) mode is higher than the no-adhesion mode. Also, the friction has a minor effect on the magnitude of the required external force. The worst-case scenario (adhesion, no friction) was used as the base case to evaluate the strength of cells against capillary forces.

The magnitude of gravity force is approximately 2.6×10^{-16} for a bacterium, which is seven orders of magnitude smaller than the required rupture force. The effect of gravity, therefore, was not included in the analysis.

Table S2 External force required to rupture bacteria for different assumptions in the simulation

	no adhesion, no friction	**adhesion, no friction**	**adhesion and friction**
External force required to rupture the bacteria (nN)	0.89	1.12	1.09

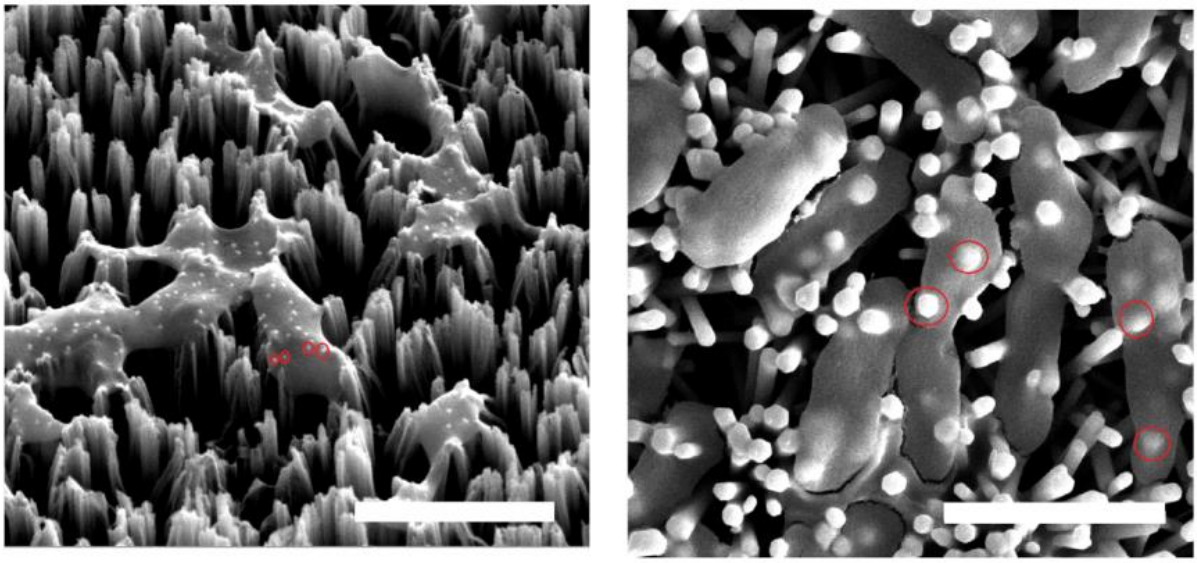

Figure S9. SEM images for estimating the number of nanopillars in contact with each bacteria. Bacteria are uncoated to make it possible to see the nanopillars (marked with red circles) penetrating through cells (scale bar = 2µm).

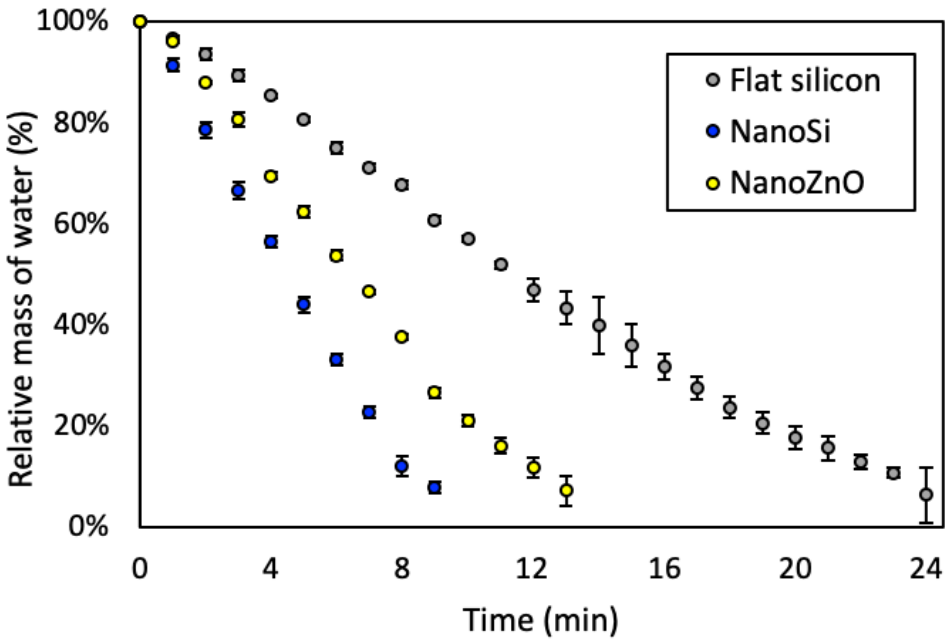

Figure S10. Droplets of water dispensed on NanoSi and NanoZnO evaporate faster respectively compared to droplets dispensed on flat silicon since the hydrophilicity of the nanotopographies greatly increase the droplet spread area.

References

1. Peng, K.; Wu, Y.; Fang, H.; Zhong, X.; Xu, Y.; Zhu, J., Uniform, axial-orientation alignment of one-dimensional single-crystal silicon nanostructure arrays. *Angewandte Chemie* **2005,** *117* (18), 2797-2802.

2. Lowder, M.; Unge, A.; Maraha, N.; Jansson, J. K.; Swiggett, J.; Oliver, J. D., Effect of Starvation and the Viable-but-Nonculturable State on Green Fluorescent Protein (GFP) Fluorescence in GFP-Tagged Pseudomonas fluorescens A506. *Applied and Environmental Microbiology* **2000,** *66* (8), 3160-3165

3. Angelini, T. E., Dunn, A. C., Urueña, J. M., Dickrell, D. J., 3rd, Burris, D. L., & Sawyer, W. G., Cell friction. *Faraday Discuss* **2012** (156*)* 31-39

4. Matias, V. R.; Al-Amoudi, A.; Dubochet, J.; Beveridge, T. J., Cryo-transmission electron microscopy of frozen-hydrated sections of Escherichia coli and Pseudomonas aeruginosa. *Journal of bacteriology* **2003,** *185* (20), 6112-6118.

5. Thwaites JJ, Surana UC., N. H., Mechanical properties of Bacillus subtilis cell walls: effects of removing residual culture medium. *J Bacteriol.* **1991** 173 (1), 197-203.

6. Yi Deng, Mingzhai Sun, and Joshua W. Shaevitz, Direct Measurement of Cell Wall Stress Stiffening and Turgor Pressure in Live Bacterial Cells. *Phys. Rev. Lett.* **2011** (107) 158101